

MUTISCALE MODEL REDUCTION FOR
DARCY-FORCHHEIMER MODEL WITH ONLINE
CORRECTION IN PERFORATED MEDIA

D.A. SPIRIDONOV.[orcid.pdf](#)

Communicated by P.P. PETROV

Abstract:In this study, we introduce an algorithm for the Darcy–Forchheimer model in perforated media using the online generalized multiscale finite element method (Online GMsFEM). A nonlinear Darcy flow with a high inertial effect and flow speed is described by the mathematical model. The finite element method (FEM) is used to perform the fine grid approximation. We employ a model reduction technique known as Online GMsFEM, which is predicated on coarse neighborhood local residuals. We employ another offline multiscale basis functions to characterize a boundary condition on perforations in the multiscale approximation. In each local domain, the online multiscale basis functions are built using residuals. The Darcy-Forchheimer equation can now account for the effects of nonlinear coefficients because to the existence of such online multiscale basis functions. We present numerical results in a two-dimensional heterogeneous perforated domain. We analyze the method’s accuracy in relation to the impact of nonlinearity. The numerical tests demonstrate the excellent accuracy of the Online GMsFEM for these kinds of

SPIRIDONOV, D.A., MUTISCALE MODEL REDUCTION FOR DARCY-FORCHHEIMER MODEL WITH ONLINE CORRECTION IN PERFORATED MEDIA.

© 2024 SPIRIDONOV D.A..

The work is supported by the grant of RCF №23-71-10074(<https://rscf.ru/project/23-71-10074/>).

Received October, 1, 2024, Published December, ??, 2024.

nonlinear problems. The accuracy weakly depends on the magnitude of the nonlinear part of the equation.

Keywords: Darcy–Forchheimer model, Online generalized multiscale finite element method, multiscale model reduction, finite element method, perforated domain, nonlinear flow problem.

Аннотация: В данной работе представлено алгоритм для модели Дарси–Форхгеймера в перфорированных средах с использованием онлайн обобщенного многомасштабного метода конечных элементов (Online GMSFEM). Нелинейный поток Дарси с высоким инерционным эффектом и скоростью потока описывается математической моделью. Метод конечных элементов (МКЭ) используется для аппроксимации мелкой сетки. Применен метод понижения порядка модели, известный как Online GMSFEM, который основан на невязках в локальных областях грубой сетки. Для учета граничного условия на перфорациях в аппроксимации на грубой сетке строятся специальные оффлайн дополнительные базисные функции. В каждой локальной области онлайн многомасштабные базисные функции строятся с использованием невязок. Уравнение Дарси–Форхгеймера теперь может учитывать эффекты нелинейных коэффициентов благодаря существованию таких онлайн многомасштабных базисных функций. Численные результаты представлены в двумерной неоднородной перфорированной области. Точность метода исследуется в зависимости от величины нелинейной части уравнения. Численные тесты демонстрируют превосходную точность Online GMSFEM для этих видов нелинейных задач. Точность слабо зависит от величины нелинейной части уравнения.

Ключевые слова: Модель Дарси–Форхгеймера, обобщенный многомасштабный метод конечных элементов, многомасштабное понижение порядка модели, метод конечных элементов, перфорированная область, нелинейная задача фильтрации.

1 Introduction

In this paper, we consider a multiscale modeling of the Darcy–Forchheimer model in a perforated medium. In nonlinear filtration problems, two cases are distinguished. This are high and low speed flows. At high speed flows, when the inertial component is significant, the Darcy–Forchheimer formula is used [?]. Fluid flow in porous media is an essential element in understanding oil and gas production processes, as well as in reservoir hydrology, environmental protection, and many other [?].

The basic law of filtration of liquids and gases in porous media is Darcy’s law; it expresses the dependence of fluid filtration rate on the pressure gradient. Many scientific works are devoted to checking and investigating the limits of the applicability of Darcy’s law [?, ?]. In cases where the

filtration rate is relatively high, inertial effects cannot be ignored, the Darcy–Forchheimer model is used [?, ?]. High filtration rates can occur in highly heterogeneous media and near perforations due to influence of boundary condition. In this paper, we consider the multiscale method for the nonlinear flow model in a perforated porous medium based on the Darcy–Forchheimer model [?].

Standard modeling approaches imply the use of well-known methods of approximation on a fine grid. One of such methods is well-proven in the field of mathematical modeling, the finite element method [?]. For modeling the Darcy–Forchheimer model, the mixed finite element method is most commonly used, providing the law of conservation of mass [?, ?]. In this paper, we use the finite element method to solve a problem on the fine grid.

One way is to solve the problem on a coarse grid. One of these methods is the homogenization method [?, ?]. In this study, we use multiscale modeling techniques to reduce the dimensionality of the original problem [?, ?]. There are many modifications of multiscale methods, each modification of the method may be suitable for a specific task. The most famous is the multiscale finite element method (MsFEM) [?, ?]. The simple MsFEM has a high error in high contrast domains. In this regard, a method was invented that allows adding more basis functions by solving spectral problems, this method is known as the generalized multiscale finite element method (GMsFEM) [?, ?, ?]. Based on the finite volume method, a multiscale finite volume method (MsFVM) was developed [?, ?]. For problems with complex heterogeneity, such as channels or fractures and perforations, multiscale methods with an oversampling strategy are well suited, one of such method is the constraint energy minimizing generalized multiscale finite element method (CEM-GMsFEM) [?, ?]. Oversampled local domains allow multiscale basis functions to take into account the influence of heterogeneity in neighboring local domains. The Darcy–Forchheimer model is often written in a mixed formulation, a mixed finite element method (Mixed-FEM) has been developed to solve such problems [?]. Another approach of multiscale modeling of Darcy–Forchheimer flow is Non-local multi-continuum method (NLMC) [?]. For nonlinear problems, the online generalized multiscale finite method (Online GMsFEM) is well suited that allows to take into account changes in properties by adding additional multiscale bases while solving the problem [?, ?, ?].

This paper considers an Online generalized multiscale finite element method (Online GMsFEM) for Darcy–Forchheimer flow in a heterogeneous perforated domain. The algorithm consists of two parts: offline and online stages. In the offline stage, we construct an offline multiscale basis functions, which do not change throughout the entire modeling process. Also, in the offline stage we calculate an additional multiscale basis functions to take into account boundary conditions on perforations. We solve the system on a coarse grid and construct a residual-based online multiscale basis functions at the online stage using the obtained bases. Note that the approximation is based on the finite element method. Numerical results are presented for a two-dimensional

perforated heterogeneous domain. The numerical experiment includes investigating the nonlinearity effects on the Online GMSFEM accuracy. We note that one can, in general, design various online approaches for nonlinear problems. Our goal is to have a simple and efficient online approach, which was proposed here.

The paper is organized as follows. Section 2 presents the Darcy–Forchheimer model in a perforated heterogeneous domain. Section 3 describes a fine grid approximation using the finite element method. Section 4 presents an algorithm of the online generalized multiscale finite element method (Online GMSFEM) for the Darcy–Forchheimer model. We provide a numerical experiment to investigate the influence of nonlinearity on the method accuracy in Section 5.

2 Problem formulation

The filtration process is described by the well-known Darcy law equation

$$\mu k^{-1}u + \nabla p = 0.$$

Let us supplement the basic equation of Darcy’s law with a nonlinear term. And we can obtain a Darcy–Forchheimer single phase flow model

$$\begin{aligned} \mu k^{-1}u + \rho\beta|u|u + \nabla p &= g, \quad x \in \Omega, \\ \nabla \cdot u &= f, \quad x \in \Omega, \end{aligned} \tag{1}$$

where p is the pressure, u is the velocity, k is the heterogeneous permeability, μ is the viscosity, ρ is the density and β is the Forchheimer coefficient. The impact of nonlinearity on the overall physical process is determined by the Forchheimer coefficient.

The system (??) is complemented with Dirchlet boundary condition,

$$p = p_D, \quad x \in \partial\Omega.$$

In the continuous level, the Darcy–Forchheimer equation can be rewritten into a nonlinear primary formulation. For simplicity, we assume that the permeability is a scalar. Taking the norm of the Darcy–Forchheimer equation, we obtain

$$\begin{aligned} (\mu k^{-1} + \rho\beta|u|)|u| &= |-\nabla p + g|, \\ \rho\beta|u|^2 + \mu k^{-1}|u| - |\nabla p - g| &= 0, \end{aligned}$$

and can solve for $|u|$

$$|u| = \frac{-\mu k^{-1} + \sqrt{(\mu k^{-1})^2 + 4\rho\beta|\nabla p - g|}}{2\rho\beta},$$

and consequently u :

$$u = -\frac{\nabla p - g}{\mu k^{-1} + \rho\beta|u|} = -\frac{2(\nabla p - g)}{\mu k^{-1} + \sqrt{(\mu k^{-1})^2 + 4\rho\beta|\nabla p - g|}}.$$

Then, substituting back to the divergence equation, we get the primary formulation of pressure p only

$$-\nabla \cdot \left(\frac{2(\nabla p - g)}{\mu k^{-1} + \sqrt{(\mu k^{-1})^2 + 4\rho\beta|\nabla p - g|}} \right) = f. \quad (2)$$

The well-posedness of primary formulation of pressure can be found in [?].

In this study, we take a dynamic nonlinear filtration process into consideration and include a temporal derivative and $g = 0$. Therefore, the dynamic incompressible single-phase Darcy–Forchheimer flow equation can be written as follows

$$c \frac{\partial p}{\partial t} - \nabla \cdot \left(\frac{2\nabla p}{\mu k^{-1} + \sqrt{(\mu k^{-1})^2 + 4\rho\beta|\nabla p|}} \right) = f. \quad (3)$$

In this paper, we consider the nonlinear filtration process in fractured media. We define the porous matrix domain as $\Omega \in \mathcal{R}^d$. In our implementation, we consider problems in the two-dimensional domain $d = 2$. And we can define the nonlinear Darcy–Forchheimer flow in a perforated domain:

$$c \frac{\partial p}{\partial t} + \nabla \cdot u = f, \quad x \in \Omega, \quad t > 0, \quad (4)$$

where,

$$u = - \frac{2\nabla p}{\mu k^{-1} + \sqrt{(\mu k^{-1})^2 + 4\rho\beta|\nabla p|}}.$$

We apply the following vounary condition for (??):

$$p = g, \quad x \in \Gamma_P, \quad p = 0, \quad x \in \partial\Omega/\Gamma_P, \quad (5)$$

and set the initial condition $p = p_0$ for $t = 0$, Γ_P is the boundary of perforations inside domain Ω .

3 Fine grid approximation

Next, we consider the fine grid approximation of the problem (??), (??). We use the finite element method with a discrete fracture model. We define unstructured triangular fine grid \mathcal{T}_h , with perforations. For the time-dependent problem, we note n as a number of time layers, τ as the time step, and $T_{max} = n\tau$ as the final time. We consider N_f as the number of elements in fine grid.

We have the following approximation on the fine grid:

$$\begin{aligned} \int_{\Omega} c \frac{\partial p}{\partial t} v \, dx + \int_{\Omega} \left(\frac{2\nabla p}{\mu k^{-1} + \sqrt{(\mu k^{-1})^2 + 4\rho\beta|\nabla p|}}, \nabla v \right) dx = \\ = \int_{\Omega} f v \, dx, \quad v \in \hat{V}, \end{aligned} \quad (6)$$

where $p \in V$ and

$$V = \{v \in H^1(\Omega) : v = g, x \in \Gamma_P, v = 0, x \in \partial\Omega/\Gamma_P\},$$

$$\hat{V} = \{v \in H^1(\Omega) : v = 0, x \in \partial\Omega\}.$$

For the approximation of the time derivative, we use the backward Euler method. To resolve non-linearity we use Picard iteration method and obtain the following approximation on the fine grid

$$\begin{aligned} \int_{\Omega} c \frac{p_{t+1}^{n+1} - p^n}{\tau} v dx + \int_{\Omega} \left(\frac{2\nabla p_{t+1}^{n+1}}{\mu k^{-1} + \sqrt{(\mu k^{-1})^2 + 4\rho\beta|\nabla p_t^{n+1}|}}, \nabla v \right) dx = \\ = \int_{\Omega} f v dx, \quad v \in \hat{V}, \end{aligned} \quad (7)$$

where t denotes a Picard iteration step. Note that p^n is no subindex t since they show a previous time iterate. We use the following termination criteria in the Picard iterations:

$$\frac{\|p_{t+1}^{n+1} - p_t^{n+1}\|_{L_2}}{\|p_{t+1}^{n+1}\|_{L_2}} < \varepsilon,$$

in our implementation, we took $\varepsilon = 10^{-3}$.

We can write approximation, in the matrix form as

$$\frac{1}{\tau} S_{t+1}^{n+1} (p_{t+1}^{n+1} - p^n) + A_t^{n+1} p_{t+1}^{n+1} = F_{t+1}^{n+1} \quad (8)$$

where S_{t+1}^{n+1} is a mass matrix that corresponds to the first term, A_t^{n+1} is a stiffness matrix that corresponds to the second nonlinear term and F_{t+1}^{n+1} is a source term in (??).

4 Coarse grid approximation

To make approximation on the coarse grid, we apply an Online Generalized Multiscale Finite Element method. A coarse grid \mathcal{T}_H is denoted by

$$\mathcal{T}_H = \bigcup_j K_j,$$

here K_j is the cell of coarse grid. Following that, we create a local coarse neighborhood domain ω_i it is produced by merging all coarse cells around one coarse grid vertex:

$$\omega_i = \bigcup_j K_j \in \mathcal{T} : x_i \in K_j,$$

where $i = \overline{1, N_c}$ and N_c – the number of coarse grid vertices.

We can identify two stages in GMSFEM, online and offline.

4.1. Offline Stage. We start from the constructing a snapshot space $V_{snap}^{\omega_i}$. The snapshot space are obtained by solving next local problems

$$\int_{\omega_i} \left(\frac{2\nabla\phi_j^i}{\mu k^{-1} + \sqrt{(\mu k^{-1})^2 + 4\rho\beta}}, \nabla w^i \right) dx = 0,$$

with boundary condition:

$$\phi_j^i = \delta_j, \quad x \in \partial\omega_i/\Gamma_P, \quad \frac{\partial\phi^i}{\partial n} = 0, \quad x \in \Gamma_P, \quad (9)$$

where δ_j is the discrete delta function which takes the value 1 at the j -th fine grid node $x = x_j$ and zero elsewhere ($j = 1, \dots, J^i$, J^i is number of fine grid nodes on boundary $\partial\omega_i$).

The snapshot space and the projection matrix on the snapshot space are defined as follows

$$V_i^{snap} = \text{span}\{\phi_1^i, \dots, \phi_{J^i}^i\}, \quad \text{and} \quad R_i^{snap} = (\phi_1^i, \dots, \phi_{J^i}^i)^T.$$

On the snapshot space we solve the next local spectral problem in each ω_i to obtain an offline multiscale basis functions

$$\tilde{A}\tilde{\Psi}_{snap,j}^i = \lambda\tilde{S}\tilde{\Psi}_{snap,j}^i,$$

with

$$\tilde{A} = R_{snap,i} A^{\omega_i} R_{snap,i}^T, \quad \tilde{S} = R_{snap,i} S^{\omega_i} R_{snap,i}^T,$$

where

$$A^{\omega_i} = \{a_{ln}\}, \quad a_{ln} = \int_{\omega_i} \left(\frac{2\nabla\psi_l}{\mu k^{-1} + \sqrt{(\mu k^{-1})^2 + 4\rho\beta}}, \nabla\psi_n \right) dx,$$

$$S^{\omega_i} = \{s_{ln}\}, \quad s_{ln} = \int_{\omega_i} \frac{2\nabla\psi_l}{\mu k^{-1} + \sqrt{(\mu k^{-1})^2 + 4\rho\beta}} \psi_n dx.$$

We use solution of the spectral problem $\Psi_j^i = R_{snap,i} \tilde{\Psi}_{snap,j}^i$ in offline basis construction. We should note that, we construct the offline multiscale basis functions only once in the offline stage. Because of that, we take $|\nabla p_t^{n+1}| = 1$ for offline bases computation. We obtain offline multiscale basis functions by multiplication on the linear partition of unity function $\psi_j^i = \chi_i \Psi_j^i$, where χ_i is the linear coarse grid nodal basis function that is equal to zero on the boundary of local domain ω_i and one at the coarse grid node i .

Now, we can determine the offline space

$$V_{ms} = \text{span}(\psi_1^1, \dots, \psi_{M_1}^1, \dots, \psi_1^{N_c}, \dots, \psi_{M_{N_c}}^{N_c}).$$

and the offline projection matrix

$$R^T = (\psi_1^1, \dots, \psi_{M_1}^1, \dots, \psi_1^{N_c}, \dots, \psi_{M_{N_c}}^{N_c}).$$

Additional offline multiscale basis functions.

Inside the computation domain Ω we have parforations. And to take into account the influence of boundary condition Γ_P we need to introduce an additional basis function in the offline stage. This function we denote as θ^i

and we calculate it only in local domains ω_i which contains perforations. Let N_P is the number of ω_i with perforations. To obtain an additional basis function we solve the next problem in ω_i with perforations:

$$\begin{aligned} -\nabla \cdot \left(\frac{2\nabla\theta^i}{\mu k^{-1} + \sqrt{(\mu k^{-1})^2 + 4\rho\beta}} \right) &= 0, \quad x \in \omega_i, \\ \theta^i &= 0, \quad x \in \partial\omega_i/\Gamma_p, \\ \theta^i &= g, \quad x \in \Gamma_p. \end{aligned} \quad (10)$$

After that, we include additional basis functions in multiscale space V_{ms} and projection matrix R :

$$\begin{aligned} V_{ms} &= \text{span}(\psi_1^1, \dots, \psi_{M_1}^1, \dots, \psi_1^{N_c}, \dots, \psi_{M_{N_c}}^{N_c}, \theta^1, \dots, \theta^{N_P}), \\ R^T &= (\psi_1^1, \dots, \psi_{M_1}^1, \dots, \psi_1^{N_c}, \dots, \psi_{M_{N_c}}^{N_c}, \theta^1, \dots, \theta^{N_P}). \end{aligned}$$

4.2. Online Stage. In online GMSFEM, we update projection matrix R^n by adding online residual based multiscale basis functions at n -th time step. Therefore, we solve next system on the coarse grid

$$S_{c,t+1}^{n+1} \frac{p_{c,t+1}^{n+1} - p_c^n}{\tau} + A_{c,t}^{n+1} p_{c,t+1}^{n+1} = F_{c,t+1}^{n+1}, \quad (11)$$

where coarse scale matrices and vectors are constructed using current projection matrix R^{n+1}

$$\begin{aligned} S_{c,t+1}^{n+1} &= R^{n+1} S_{t+1}^{n+1} (R^{n+1})^T, \quad A_{c,t}^{n+1} = R^{n+1} A_t^{n+1} (R^n)^T, \\ F_{c,t+1}^{n+1} &= R^{n+1} F_{t+1}^{n+1}, \quad p_{ms}^{n+1} = (R^{n+1})^T p_c^{n+1}. \end{aligned}$$

Note that, when we use pre-constructed offline multiscale basis functions for given heterogeneity and fracture distribution in coarse scale system construction, we can use predefined projection matrix without updating it at n -th time step

$$(R^n)^T = R^T = (\psi_1^1, \dots, \psi_{M_1}^1, \dots, \psi_1^{N_c}, \dots, \psi_{M_{N_c}}^{N_c}, \theta^1, \dots, \theta^{N_P}).$$

In online GMSFEM, we set $R^n = R$ at first time step ($n = 0$), then we construct and solve coarse scale system (??). Next, at time step $n = 1, 2, \dots$, we enrich multiscale space by residual based online multiscale basis functions. In order to enrich space, we solve system (??) with $R^n = R^{n-1}$, then we calculate online multiscale basis functions ϑ_1^i locally in ω_i using current residuals and update the projection matrix

$$(R^{1,n})^T = (\psi_1^1, \dots, \psi_{M_1}^1, \dots, \psi_1^{N_c}, \dots, \psi_{M_{N_c}}^{N_c}, \vartheta_1^1, \dots, \vartheta_1^{N_c}).$$

We can reiterate the process with residual calculation and add more online basis functions on the n th time step

$$\begin{aligned} (R^n)^T &= (R^{L,n})^T = (\psi_1^1, \dots, \psi_{M_1}^1, \dots, \psi_1^{N_c}, \dots, \psi_{M_{N_c}}^{N_c}, \theta^1, \dots, \theta^{N_P}, \\ &\quad \vartheta_1^1, \dots, \vartheta_1^{N_c}, \dots, \vartheta_L^1, \dots, \vartheta_L^{N_c}), \end{aligned}$$

where L is the number of online iterations. We can enrich multiscale space not for every time steps, for example, every 4-th. Then, when we keep R^n for the time steps where we do not want to update online basis functions. Next, we present construction of the online multiscale basis functions in local domain ω_i in details.

Construction of the local residual based online multiscale basis functions is based on the solution of the following local problem in ω_i :

$$a_{\omega_i}(\vartheta_l^i, v) = r_{\omega_i}^l(v), \quad l = 1, \dots, L,$$

where

$$\begin{aligned} a_{\omega_i}(\vartheta_l^i, v) &= \int_{\omega_i} c \frac{\vartheta_l^i}{\tau} v \, dx + \int_{\omega_i} \left(\frac{2\nabla \vartheta_l^i}{\mu k^{-1} + \sqrt{(\mu k^{-1})^2 + 4\rho\beta|\nabla p_{ms,t+1}^{l,n+1}|}}, \nabla v \right) dx + \\ r_{\omega_i}^l(v) &= \int_{\omega_i} f v \, dx - \int_{\omega_i} c \frac{p_{ms,t+1}^{l,n+1} - p_{ms}^{l,n}}{\tau} v \, dx - \\ &\quad - \int_{\omega_i} \left(\frac{2\nabla p_{ms,t+1}^{l,n+1}}{\mu k^{-1} + \sqrt{(\mu k^{-1})^2 + 4\rho\beta|\nabla p_{ms,t+1}^{l,n+1}|}}, \nabla v \right) dx \end{aligned}$$

with the following Dirichlet boundary conditions:

$$\vartheta_l^i = 0, \quad x \in \partial\omega_i/\Gamma_P, \quad \vartheta_l^i = g, \quad x \in \Gamma_P. \quad (12)$$

Using constructed online multiscale basis functions, we enrich the multiscale space by adding online basis functions ϑ_l^i :

$$V_{ms} = \text{span}(\psi_1^i, \dots, \psi_{M_i}^i, \theta^1, \dots, \theta^{N_P}, \vartheta_1^1, \dots, \vartheta_1^{N_c}, i = 1, \dots, N_c, l = 1, \dots, L).$$

Here we can add several online multiscale basis functions in local domain ω_i based on the current solution $p_{ms}^{l,n}$

$$S_{c,t+1}^{l,n+1} \frac{p_{c,t+1}^{l,n+1} - p_c^n}{\tau} + A_{c,t}^{l,n} p_{c,t+1}^{l,n+1} = F_{c,t+1}^{l,n+1},$$

where coarse scale matrices and vectors are constructed using current projection matrix $R^{l,n}$

$$S_{c,t+1}^{l,n+1} = R^{l,n+1} S_{t+1}^n (R^{l,n+1})^T, \quad A_{c,t}^{l,n+1} = R^{l,n+1} A_t^{n+1} (R^{l,n+1})^T,$$

$$F_{c,t+1}^{l,n+1} = R^{l,n+1} F_{t+1}^{n+1}, \quad p_{ms,t+1}^{l,n+1} = (R^{l,n+1})^T p_{c,t+1}^{l,n+1}.$$

with projection matrix

$$R^{l,n+1} = (\psi_1^1, \dots, \psi_{M_1}^1, \dots, \psi_1^{N_c}, \dots, \psi_{M_{N_c}}^{N_c}, \theta^1, \dots, \theta^{N_P}, \vartheta_1^1, \dots, \vartheta_1^{N_c}, \dots, \vartheta_l^1, \dots, \vartheta_l^{N_c})^T,$$

where $l = 1, \dots, L$, $R^{n+1} = R^{L,n+1}$, and L is the number of the online iterations.

5 Numerical results

In this section, we use Online GMSFEM to provide numerical results for the Darcy–Forchheimer problem. We consider the flow problem in the two-dimensional perforated heterogeneous domain. We show the heterogeneous coefficient k_m in Figure ??.

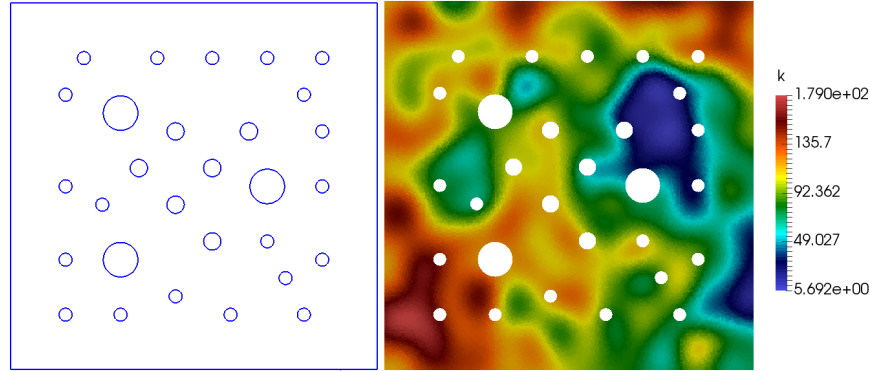


FIG. 1. Heterogeneity and computational domain Ω . Left: computational domain Ω . Right: Coefficient k_m .

We consider numerical experiments for coarse grid 10×10 and fine grid with 14649 vertices. We consider results with different values of β to investigate the effect of nonlinearity. In the implementation, we consider results for $\beta = 10^5, \beta = 10^4, \beta = 10^3, \beta = 10^2, \beta = 10$. And we take maximum time $T_{max} = 1.5, T_{max} = 0.5, T_{max} = 0.17, T_{max} = 0.05, T_{max} = 0.017$ respectively for each value of β and we use 20 time layers for each test case. We set $\mu = 1.0, \rho = 1.0, c = 1.0, f = 0$. We put Dirichlet boundary condition on perforations $p = g, g = 1.0$ and zero Dirichlet boundary on the all external boundaries of Ω . To investigate the accuracy of the Online GMSFEM algorithm, we compare the multiscale solutions with the reference solutions. We take a fine-grid solution as a reference solution. The fine grid system’s size equals 14649×14649 .

We compare solutions by using L_2 and H_1 norm errors

$$e^{L_2} = \sqrt{\frac{\int_{\Omega} (p_f - p_{ms})^2 dx}{\int_{\Omega} p_f^2 dx}} \cdot 100\%, \quad e^{H_1} = \sqrt{\frac{\int_{\Omega} (\nabla(p_f - p_{ms}))^2 dx}{\int_{\Omega} (\nabla p_f)^2 dx}} \cdot 100\%,$$

where p_{ms} is the multiscale solution, p_f is the solution on the fine grid.

The numerical results are presented in Fig. ?? for $\beta = 10^5$. The first row shows a solution on a fine grid, the second row shows a solution using GMSFEM using only 12 offline multiscale basis functions without online correction, the third row shows a solution using Online GMSFEM using 12 offline multiscale basis functions and 2 online multiscale basis function. We present solutions for the 2-nd, 10-th, and final time layers to demonstrate

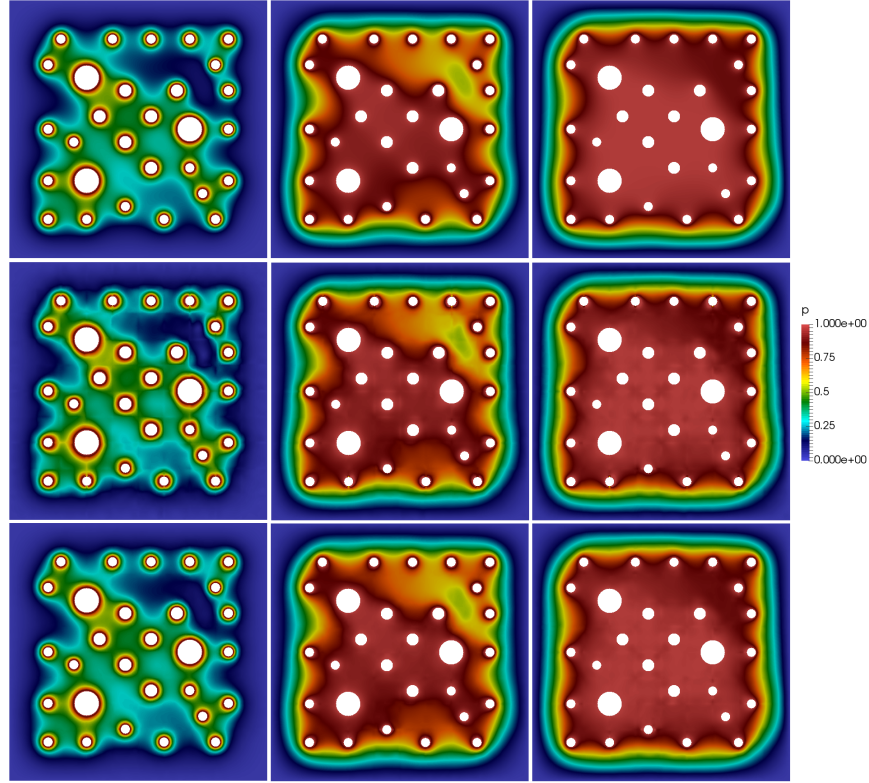


FIG. 2. Numerical results for $\beta = 10^5$ at the 2-nd, 10-th, and last time layer. First row: fine grid solution. Second row: multiscale solution on using only 12 offline multiscale basis functions. Third row: multiscale solution on using 12 offline multiscale basis functions and 2 online multiscale basis function.

time distribution. In the figures, we can see small oscillations in the offline GMsFEM solution near perforations. Online GMsFEM solution and fine grid solution looks very similar, in the Online GMsFEM solution we don't see any oscillations.

We present relative L_2 and H_1 errors in Tables ??-?? for multiscale solution using 0, 1, and 2 online basis functions for different number of offline basis functions. In the tables, DOF_c denotes the vector size on the coarse grid. By this tables we can see that, the accuracy behavior is similar for all values of β . In all test cases, when we use 12 offline and 1 online basis functions we can obtain a solution with accuracy good accuracy. But, without online correction, we can't achieve high accuracy, we have very large value of H_1 error. We can conclude that it is necessary to use online correction in this problem. Using online basis functions, we can obtain a solution using a system with a smaller number of unknowns. Adding a second online basis in

| Number of offline basis functions | Offline basis | | | 1 Online basis | | | 2 Online basis | | |
|---|---------------|-----------|-----------|----------------|-----------|-----------|----------------|-----------|-----------|
| | DOF_c | e^{L_2} | e^{H_1} | DOF_c | e^{L_2} | e^{H_1} | DOF_c | e^{L_2} | e^{H_1} |
| 1 | 202 | 5.951 | 76.667 | 323 | 6.289 | 48.488 | 444 | 3.145 | 33.133 |
| 2 | 323 | 5.281 | 73.391 | 444 | 5.525 | 45.693 | 565 | 2.777 | 31.578 |
| 4 | 569 | 3.054 | 54.298 | 686 | 2.847 | 29.362 | 806 | 1.872 | 22.797 |
| 6 | 807 | 2.731 | 52.331 | 928 | 2.241 | 24.967 | 1049 | 1.538 | 19.927 |
| 8 | 1049 | 2.249 | 50.524 | 1170 | 1.717 | 21.179 | 1291 | 1.271 | 17.653 |
| 12 | 1533 | 2.026 | 49.641 | 1654 | 1.357 | 18.943 | 1775 | 0.962 | 15.971 |
| 16 | 2017 | 1.905 | 49.065 | 2138 | 1.093 | 17.201 | 2259 | 0.741 | 14.418 |
| 24 | 2985 | 1.788 | 48.412 | 3106 | 0.807 | 14.874 | 3227 | 0.568 | 12.541 |
| 32 | 3953 | 1.756 | 48.348 | 4074 | 0.743 | 14.481 | 4195 | 0.492 | 12.014 |

TABLE 1. Numerical results for $\beta = 10$. Relative L_2 and $H_1(\%)$ errors with different number of offline multiscale basis functions using 1 and 2 online basis functions on the last time layer.

| Number of offline basis functions | Offline basis | | | 1 Online basis | | | 2 Online basis | | |
|---|---------------|-----------|-----------|----------------|-----------|-----------|----------------|-----------|-----------|
| | DOF_c | e^{L_2} | e^{H_1} | DOF_c | e^{L_2} | e^{H_1} | DOF_c | e^{L_2} | e^{H_1} |
| 1 | 202 | 6.261 | 76.274 | 323 | 5.879 | 48.605 | 444 | 3.481 | 31.172 |
| 2 | 323 | 5.251 | 73.037 | 444 | 5.561 | 45.345 | 565 | 3.165 | 29.598 |
| 4 | 569 | 3.007 | 53.975 | 686 | 2.875 | 29.548 | 806 | 1.874 | 22.111 |
| 6 | 807 | 2.688 | 52.035 | 928 | 2.254 | 24.811 | 1049 | 1.529 | 19.268 |
| 8 | 1049 | 2.234 | 50.272 | 1170 | 1.731 | 21.063 | 1291 | 1.251 | 17.106 |
| 12 | 1533 | 2.024 | 49.389 | 1654 | 1.361 | 18.796 | 1775 | 0.967 | 15.435 |
| 16 | 2017 | 1.917 | 48.821 | 2138 | 1.098 | 17.029 | 2259 | 0.767 | 13.946 |
| 24 | 2985 | 1.801 | 48.179 | 3106 | 0.808 | 14.741 | 3227 | 0.565 | 12.299 |
| 32 | 3953 | 1.777 | 48.124 | 4074 | 0.747 | 14.361 | 4195 | 0.497 | 11.745 |

TABLE 2. Numerical results for $\beta = 10^2$. Relative L_2 and $H_1(\%)$ errors with different number of offline multiscale basis functions using 1 and 2 online basis functions on the last time layer.

each ω_i improves the accuracy of the method very slightly. Overall, we can improve the accuracy of the method by about 4 times.

We need to discuss the results of the numerical experiment. We were able to prove that the proposed algorithm of the Online GMSFEM has good accuracy in all performed calculations. The method showed good accuracy in a highly heterogeneous perforated domain. The accuracy of the method is practically independent of the influence of the nonlinear part of the equation. An online correction procedure greatly improve the accuracy of the method.

| Number of offline basis functions | Offline basis | | | 1 Online basis | | | 2 Online basis | | |
|---|---------------|-----------|-----------|----------------|-----------|-----------|----------------|-----------|-----------|
| | DOF_c | e^{L_2} | e^{H_1} | DOF_c | e^{L_2} | e^{H_1} | DOF_c | e^{L_2} | e^{H_1} |
| 1 | 202 | 5.991 | 76.613 | 323 | 6.294 | 48.657 | 444 | 3.933 | 32.897 |
| 2 | 323 | 5.355 | 73.374 | 444 | 5.592 | 45.477 | 565 | 3.619 | 31.598 |
| 4 | 569 | 3.077 | 54.225 | 686 | 2.868 | 29.411 | 806 | 2.029 | 23.141 |
| 6 | 807 | 2.731 | 52.258 | 928 | 2.255 | 24.944 | 1049 | 1.631 | 19.862 |
| 8 | 1049 | 2.252 | 50.471 | 1170 | 1.721 | 21.161 | 1291 | 1.307 | 17.552 |
| 12 | 1533 | 2.032 | 49.568 | 1654 | 1.357 | 18.925 | 1775 | 1.011 | 15.736 |
| 16 | 2017 | 1.918 | 49.004 | 2138 | 1.102 | 17.212 | 2259 | 0.811 | 14.172 |
| 24 | 2985 | 1.789 | 48.341 | 3106 | 0.813 | 14.865 | 3227 | 0.593 | 12.501 |
| 32 | 3953 | 1.761 | 48.277 | 4074 | 0.746 | 14.463 | 4195 | 0.528 | 11.934 |

TABLE 3. Numerical results for $\beta = 10^3$. Relative L_2 and H_1 (%) errors with different number of offline multiscale basis functions using 1 and 2 online basis functions on the last time layer.

| Number of offline basis functions | Offline basis | | | 1 Online basis | | | 2 Online basis | | |
|---|---------------|-----------|-----------|----------------|-----------|-----------|----------------|-----------|-----------|
| | DOF_c | e^{L_2} | e^{H_1} | DOF_c | e^{L_2} | e^{H_1} | DOF_c | e^{L_2} | e^{H_1} |
| 1 | 202 | 5.911 | 76.307 | 323 | 6.256 | 48.572 | 444 | 4.312 | 35.833 |
| 2 | 323 | 5.294 | 73.099 | 444 | 5.586 | 45.344 | 565 | 4.032 | 34.681 |
| 4 | 569 | 3.028 | 54.005 | 686 | 2.892 | 29.594 | 806 | 2.182 | 24.134 |
| 6 | 807 | 2.701 | 52.059 | 928 | 2.271 | 24.858 | 1049 | 1.757 | 20.488 |
| 8 | 1049 | 2.243 | 50.305 | 1170 | 1.737 | 21.094 | 1291 | 1.378 | 17.875 |
| 12 | 1533 | 2.031 | 49.394 | 1654 | 1.366 | 18.814 | 1775 | 1.061 | 15.862 |
| 16 | 2017 | 1.929 | 48.845 | 2138 | 1.114 | 17.111 | 2259 | 0.848 | 14.209 |
| 24 | 2985 | 1.804 | 48.184 | 3106 | 0.815 | 14.763 | 3227 | 0.617 | 12.504 |
| 32 | 3953 | 1.778 | 48.118 | 4074 | 0.751 | 14.371 | 4195 | 0.543 | 11.936 |

TABLE 4. Numerical results for $\beta = 10^4$. Relative L_2 and H_1 (%) errors with different number of offline multiscale basis functions using 1 and 2 online basis functions on the last time layer.

The method obtains the exact solution on a coarser grid. Moreover, the dimension of the original system differs significantly. From here, we can notice significant savings in computational resources, which is the main advantage of multiscale methods over standard mathematical modeling approaches.

| Number of offline basis functions | Offline basis | | | 1 Online basis | | | 2 Online basis | | |
|---|---------------|-----------|-----------|----------------|-----------|-----------|----------------|-----------|-----------|
| | DOF_c | e^{L_2} | e^{H_1} | DOF_c | e^{L_2} | e^{H_1} | DOF_c | e^{L_2} | e^{H_1} |
| 1 | 202 | 5.888 | 76.288 | 323 | 6.102 | 48.208 | 444 | 4.517 | 39.052 |
| 2 | 323 | 5.273 | 73.083 | 444 | 5.455 | 45.082 | 565 | 4.224 | 37.937 |
| 4 | 569 | 2.996 | 53.986 | 686 | 2.882 | 29.519 | 806 | 2.288 | 25.371 |
| 6 | 807 | 2.671 | 52.044 | 928 | 2.312 | 25.356 | 1049 | 1.858 | 21.651 |
| 8 | 1049 | 2.212 | 50.291 | 1170 | 1.763 | 21.559 | 1291 | 1.439 | 18.765 |
| 12 | 1533 | 1.996 | 49.376 | 1654 | 1.393 | 19.404 | 1775 | 1.117 | 16.879 |
| 16 | 2017 | 1.901 | 48.838 | 2138 | 1.156 | 17.913 | 2259 | 0.911 | 15.478 |
| 24 | 2985 | 1.771 | 48.168 | 3106 | 0.871 | 15.695 | 3227 | 0.713 | 13.892 |
| 32 | 3953 | 1.742 | 48.086 | 4074 | 0.813 | 15.339 | 4195 | 0.653 | 13.477 |

TABLE 5. Numerical results for $\beta = 10^5$. Relative L_2 and H_1 (%) errors with different number of offline multiscale basis functions using 1 and 2 online basis functions on the last time layer.

6 Conclusion

This paper presents an Online generalized multiscale finite element method (Online GMsFEM) algorithm for the time-dependent Darcy-Forchheimer model in a perforated heterogeneous domain. We construct the fine grid approximation using the finite element method. Model and method formulations were given for two-dimensional cases. We investigated nonlinearity's impact by varying the coefficient β in the numerical experiments. The numerical experiment showed that the proposed approach provided accurate results without significant influence of the nonlinear part of the flow. We considered a multiscale method with different numbers of offline and online basis functions. Our experiments showed that online-correction procedure significantly reduces the error of the method, especially in H_1 norm. Adding 2-nd online basis functions gives very little improvement in the accuracy, from here we conclude that, it is not necessary to use the 2-nd online basis. The performed numerical experiment showed good accuracy of the method. We conclude that the proposed algorithm of Online generalized multiscale finite element method performed well in modeling the Darcy-Forchheimer model in the perforated medium.

References

- [1] D.G. Northcott, *Ideal Theory*, Cambridge University Press, Cambridge, 1953.
- [2] I.I. Ivanov, *Some properties of commutative algebras*, Siberian Electronic Mathematical Reports, **1** (2004), 142–143.
- [3] A.V. Tetenov, M. Samuel, D.A. Vauilin, *On dendrites generated by polyhedral systems and their ramification points*, Trudy Inst. Mat. Mekh. UrO RAN, **23:4** (2017), 281–291.

- [4] V. Girault, M.F. Wheeler, *Numerical discretization of a Darcy–Forchheimer model*, Numerische Mathematik, **110**:2 (2008), 161–198.
- [5] A. Cescon, J.Q. Jiang, *Filtration process and alternative filter media material in water treatment*, Water, **12**:12 (2020), 3377.
- [6] U.S. Gavriliava, V.N. Alekseev, M.V. Vasil’eva, *Flow and transport in perforated and fractured domains with robin boundary conditions*, Mathematical notes of NEFU, **24**:3 (2017), 65–77.
- [7] D.Y. Nikiforov, S.P. Stepanov, *Numerical simulation of the embedded discrete fractures by the finite element method*, Journal of Physics: Conference Series, **1158** (2019), 032038 .
- [8] M.I. Khan, F. Alzahrani, A. Hobiny, *Simulation and modeling of second order velocity slip flow of micropolar ferrofluid with Darcy–Forchheimer porous medium*, Journal of Materials Research and Technology, **9**:4 (2020), 7335–7340.
- [9] Y. Chu, M.I. Khan, M.I.U. Rehman, S. Kadry, S. Qayyum, M. Waqas, *Stability analysis and modeling for the three-dimensional Darcy–Forchheimer stagnation point nanofluid flow towards a moving surface*, Applied Mathematics and Mechanics, **42**:3 (2021), 357–370.
- [10] G. Dhatt, E. Lefrançois, G. Touzot, *Finite element method*, John Wiley and Sons, 2012.
- [11] J. Huang, L. Chen, H. Rui, *Multigrid methods for a mixed finite element method of the Darcy–Forchheimer model*, Journal of Scientific Computing, **74** (2018), 396–411.
- [12] W. Xu, D. Liang, H. Rui, *A multipoint flux mixed finite element method for the compressible Darcy–Forchheimer models*, Applied Mathematics and Computation, **315** (2017), 259–277.
- [13] S.P. Stepanov, D.A. Spiridonov, T. Mai, *Prediction of numerical homogenization using deep learning for the Richards equation*, Journal of Computational and Applied Mathematics, **424** (2023), 114980.
- [14] A.A. Tyrylgina, D.A. Spiridonov, M.V. Vasilyeva, *Numerical homogenization for poroelasticity problem in heterogeneous media*, Journal of Physics: Conference Series, **1158** (2019), 042030.
- [15] Y. Efendiev, T.Y. Hou, *Multiscale finite element methods: theory and applications*, Springer Science and Business Media, **4** 2009.
- [16] G. Allaire, R. Brizzi, *A multiscale finite element method for numerical homogenization*, Multiscale Modeling and Simulation, **4**:3 (2005), 790–812.
- [17] A. Masud, R.A. Khurram, *A multiscale finite element method for the incompressible Navier–Stokes equations*, Computer Methods in Applied Mechanics and Engineering, **195**:13-16 (2006), 1750–1777.
- [18] T.Y. Hou , X.H. Wu, *A multiscale finite element method for elliptic problems in composite materials and porous media*, Journal of Computational Physics, **134**:1 (1997), 169–189.
- [19] Y. Efendiev, J. Galvis, T.Y. Hou, *Generalized multiscale finite element methods (gmsfem)*, Journal of Computational Physics, **251** (2013), 116–135.
- [20] D.A. Spiridonov, M.V. Vasilyeva, W.T. Leung, *A generalized multiscale finite element method (gmsfem) for perforated domain flows with Robin boundary conditions*, Journal of Computational and Applied Mathematics, **357** (2019), 319–328.
- [21] D.A. Spiridonov, M.V. Vasilyeva, E.T. Chung, *Generalized multiscale finite element method for multicontinua unsaturated flow problems in fractured porous media*, Journal of Computational and Applied Mathematics, **370** (2020), 112594.
- [22] M.V. Vasilyeva, D.A.Spiridonov, *Multiscale Model Reduction with Local Online Correction for Polymer Flooding Process in Heterogeneous Porous Media*, Mathematics, **11**:14 (2023), 3104.

- [23] I. Sokolova, M.G. Bastisya, H. Hajibeygi, *Multiscale finite volume method for finite-volume-based simulation of poroelasticity*, Journal of Computational Physics, **379** (2019), 309–324.
- [24] E.T. Chung, Y. Efendiev, W.T. Leung, *Constraint energy minimizing generalized multiscale finite element method*, Computer Methods in Applied Mechanics and Engineering, **339** (2018), 298–319.
- [25] S.W. Cheung, E.T. Chung, Y. Efendiev, W.T. Leung, M.V. Vasilyeva, *Constraint energy minimizing generalized multiscale finite element method for dual continuum model*, Communications in Mathematical Sciences, **18**:3 (2020), 663–685.
- [26] D.A. Spiridonov, M.V. Vasilyeva, M. Wang, E.T. Chung, *Mixed generalized multiscale finite element method for flow problem in thin domains*, Journal of Computational and Applied Mathematics, **416** (2022), 114577.
- [27] D.A. Spiridonov, M.V. Vasilyeva, *Non-local multi-continuum method (nlmc) for Darcy–Forchheimer flow in fractured media*, Journal of Computational and Applied Mathematics, **438** (2024), 115574.
- [28] D.A. Spiridonov, S.P. Stepanov, V.I. Vasil’ev, *An online generalized multiscale finite element method for heat and mass transfer problem with artificial ground freezing*, Journal of Computational and Applied Mathematics, **417** (2023), 114561.
- [29] D.A. Spiridonov, M.V. Vasilyeva, A.A. Tyrylgina, E.T. Chung, *An online generalized multiscale finite element method for unsaturated filtration problem in fractured media*, Mathematics, **9**:12 (2021), 1382.
- [30] E.T. Chung, Y. Efendiev, W.T. Leung, *Residual-driven online generalized multiscale finite element methods*, Journal of Computational Physics, **302** (2015), 176–190.
- [31] H. Pan, H. Rui, *Mixed element method for two-dimensional Darcy–Forchheimer model*, Journal of Scientific Computing, **52** (2012), 563–587.

SPIRIDONOV DENIS ALEKSEEVICH
NORTH-EASTERN FEDERAL UNIVERSITY,
ST. BELINSKOGO 58,
677000, YAKUTSK, RUSSIA
E-mail address: d.stalnov@mail.ru